

Hypoxia-induced circCCDC66 promotes the tumorigenesis of colorectal cancer via the miR-3140/autophagy pathway

JIN FENG¹, ZHONG LI¹, LING LI¹, HAIBIN XIE¹, QICHENG LU¹ and XIAOZHOU HE²

Departments of ¹Gastrointestinal Surgery and ²Urology Surgery,
The First People's Hospital of Changzhou, Changzhou, Jiangsu 213029, P.R. China

Received November 19, 2019; Accepted July 3, 2020

DOI: 10.3892/ijmm.2020.4747

Abstract. Circular RNAs (circRNAs) have been reported to be involved in the progression of colorectal cancer (CRC). However, the biological role of circCCDC66 in CRC remains unclear. Therefore, the present study aimed to elucidate the mechanisms through which circCCDC66 affects the hypoxia-induced progression of CRC. It was found that hypoxia promoted the progression of CRC and upregulated the expression of circCCDC66. Furthermore, circCCDC66-knockdown reduced viability, migration and invasion, and enhanced the apoptosis of hypoxia-exposed CRC cells. Using the starBase database, it was identified that circCCDC66 may bind to miR-3140. Subsequently, it was confirmed that circCCDC66 serves as a sponge of miR-3140 and the depletion of miR-3140 partly abolished the effects of circCCDC66 on the phenotype of hypoxia-exposed CRC cells. In addition, miR-3140 was validated to inhibit the autophagy pathway. The use of an autophagy inducer partially reversed the miR-3140 overexpression-induced inhibition of the viability and invasion, and the promotion of the apoptosis of hypoxia-exposed CRC cells. In summary, the findings of the present study demonstrated that circCCDC66 facilitates the development of CRC cells under hypoxic conditions via regulation of miR-3140/autophagy. These findings may provide a novel therapeutic option for patients with CRC.

Introduction

Colorectal cancer (CRC) is the third most prevalent malignant neoplasm and one of the leading causes of cancer-associated mortality worldwide (1,2). Despite great efforts dedicated to therapeutic improvements, the prognosis of patients with CRC remains far from satisfactory (3,4). Hypoxia is a hallmark of the microenvironment and contributes to tumor progression and metastasis in various types of cancer, including CRC. For example, hypoxia has been shown to promote the metastasis of CRC by upregulating GDF15 expression (5). Hypoxia also facilitates epithelial-mesenchymal transition in CRC cells by regulating USP47 (6). Accordingly, it is imperative to elucidate the mechanisms governing CRC and the function of hypoxia in CRC.

Circular RNAs (circRNAs) are a category of non-coding RNA transcripts with circular configuration, which originate from exonic, intronic and intergenic regions (7,8). There is ample evidence to indicate that circRNAs are involved in the regulation of various biological activities of malignant tumors. For example, circRNA_00580631 has been shown to promote tumorigenesis of bladder cancer by sponging miR-486-3p and targeting FOXP4 (9). circRNA MTO1 inhibits gastric carcinoma progression via targeting the miR-3200-5p/PEBP1 axis (10). circRNA_103809 functions as a competing endogenous RNA (ceRNA) to promote the proliferation and migration of CRC cells by targeting the miR-532-3p/FOXO4 axis (11). circHIPK3 acts as a sponge of miR-7 to facilitate CRC growth and metastasis (12). It has been reported that circCCDC66 is upregulated in colon cancer and promotes the growth and metastasis of colon cancer (13). In addition, several studies have demonstrated that circRNAs are associated with hypoxia-mediated progression of various cancers, such as bladder cancer and breast cancer (14,15). However, the role and molecular mechanisms of circCCDC66 in hypoxia-induced CRC remain largely unknown.

MicroRNAs (miRNAs or miRs) are a type of short non-coding RNA that comprise 18-25 nucleotides and are involved in the development and evolution of multiple diseases (16,17). The dysregulation of miRNAs has been justified in a wide range of cancers and miRNAs function as oncogenes or tumor suppressors via the modulation of cellular processes, such as cell viability, apoptosis, migration, invasion and differentiation (18-20). miR-3140 has been reported to inhibit tumor

Correspondence to: Dr Xiaozhou He, Department of Urology Surgery, The First People's Hospital of Changzhou, 185 Juqian Street, Changzhou, Jiangsu 213029, P.R. China
E-mail: xiaozhouhe59@163.com

Dr Qicheng Lu, Department of Gastrointestinal Surgery, The First People's Hospital of Changzhou, 185 Juqian Street, Changzhou, Jiangsu 213029, P.R. China
E-mail: qichenglu666@126.com

Key words: colorectal cancer, circCCDC66, microRNA-3140, autophagy, hypoxia

growth *in vivo* or *in vitro* (21). Nevertheless, whether miR-3140 is involved in CRC remains to be further clarified.

In the present study, the specific function of circCCDC66 in CRC under hypoxic conditions was investigated and it was found that circCCDC66 promoted the malignant behaviors of hypoxia-exposed CRC cells by regulating the miR-3140/autophagy pathway. These findings may provide insight into the development of more effective therapeutic strategies for patients with CRC.

Materials and methods

Clinical specimens. The CRC tissues were collected from 29 patients (19 males and 10 females; 13 stage I-II and 16 stage III-IV) with a median age of 47 years (range, 31-79 years) between May 2015 and August 2018 at the First People's Hospital of Changzhou. Written informed consent was obtained from all patients prior to the study start. All tissue samples were obtained and immediately stored at -80°C prior to further experiments. The present study was approved by the First People's Hospital of Changzhou.

Cell culture and treatment. The human CRC cell lines (HCT116 and SW620), human colon mucosal cells (NCM460) and 293T cells were purchased from the American Type Culture Collection (ATCC) and maintained in DMEM (Gibco; Thermo Fisher Scientific, Inc.) with 10% FBS (Gibco; Thermo Fisher Scientific, Inc.), 100 $\mu\text{g}/\text{ml}$ streptomycin and 100 U/ml penicillin. Cells in the normoxia group were incubated at 37°C with 95% atmospheric air and 5% CO_2 at 6 l/min for 4 h. Cells in the hypoxia group were incubated at 37°C in 94% N_2 , 5% CO_2 and 1% O_2 at 6 l/min for 4 h.

Cell transfection. The short hairpin RNAs (shRNAs) targeting circCCDC66 (sh-circCCDC66) with the negative control (sh-NC), miR-3140 mimic with the negative control (NC mimic) and miR-3140 inhibitor with the negative control (NC inhibitor) were synthesized by GenePharma (Shanghai, China). Transfection was conducted with Lipofectamine 2000 transfection reagent (Invitrogen; Thermo Fisher Scientific, Inc.) according to the manufacturer's instructions.

Cell counting Kit-8 (CCK-8) assay. Following transfection, 3×10^3 cells/well were seeded into 96-well plates and then cultured at 37°C . At 0, 24, 48 and 72 h, each well was supplemented with 10 μl CCK-8 reagent (Dojindo Molecular Technologies, Inc.) and incubated for a further 4 h. The absorbance was examined at 450 nm using a microplate reader (Molecular Devices LLC).

Flow cytometric analysis. HCT116 and SW620 cells were collected with trypsin and rinsed twice using cold PBS, stained with Annexin V for 10 min in the dark and then treated with PI for 5 min, according to the manufacturer's recommendations (BD Biosciences). Following the addition of Annexin V-binding buffer, apoptotic cells were detected with a FACSCalibur flow cytometer (BD Biosciences) and analyzed using FlowJo software (version 7.5, TreeStar). The upper right and low right segments of the flow cytometry dot plots were counted to determine the level of apoptotic cells.

Wound healing assay. The migratory ability of the cells was evaluated by a wound healing assay. Cells were seeded into 6-well plates and grown until 100% confluent. Subsequently, a scratch wound was produced with a sterile 200- μl pipette tip and the cell debris was washed away using PBS. Cells were incubated in 1% FBS-supplemented DMEM for an additional 24 h. The scratch wound was observed at 0 and 24 h following incubation. Images were captured in randomly selected view fields under an Olympus CX31 microscope (Olympus Corporation) and analyzed using ImageJ software (version 1.48, National Institutes of Health).

Transwell assay. Cell invasion was assessed by a Transwell assay. A total of 5×10^5 cells and 200 μl serum-free DMEM were plated into the upper chamber of a Matrigel-coated 8- μm pore membrane (BD Biosciences). The bottom chamber was supplemented with 600 μl DMEM with 10% FBS. Following 24 h of incubation, cells in the upper chamber were removed using a cotton swab. The invaded cells were fixed by 70% ethanol, stained with 0.1% crystal violet and counted in five random fields using a light microscope (Nikon Corporation; magnification, x200).

Quantitative real-time polymerase chain reaction (RT-qPCR). Total RNA from tissues and cell lines was extracted by using TRIzol reagent (Invitrogen; Thermo Fisher Scientific, Inc.) according to the manufacturer's instructions. Reverse transcription (RT) was conducted by using the Takara PrimeScript Kit (Takara) at 37°C for 15 min. Subsequently, the RT-quantitative (q)PCR assay was performed with the ViiATM 7 Real-Time PCR System (Thermo Fisher Scientific, Inc.) to detect the gene expression level. Relative gene expression was calculated using the $2^{-\Delta\Delta\text{Ct}}$ method (22). GAPDH and U6 were set as internal controls. The PCR amplification reaction was carried out using cDNA as template with the following conditions: 95°C for 10 min, 95°C for 15 sec, 62°C for 30 sec, and 72°C for 30 sec. Primers used for PCR are as follows: circCCDC66 forward, 5'-ACCTACAACCGGAAGCCAG-3' and reverse, 5'-AGCAGTACTGTTTCCTGATGC-3'; miR-3140 forward, 5'-CTTCCACTCGACGTGCTGGAAGT-3' and reverse, 5'-ACGGTCTCGTGCAGTCGTCAACG-3'; Beclin1 forward, 5'-ACCGTGTACCATCCAGGAA-3' and reverse, 5'-GAA GCTGTTGGCACTTTCTGT-3'; p62 forward, 5'-GCAGAA TGCCATGGTTTCCC-3' and reverse, 5'-GTGATGGCTCCC CTTAC-3'; HIF1A forward, 5'-TATGAGCCAGAAGAAGCTT TAGGC-3' and reverse, 5'-CACCTCTTTTGGCAAGCA TCCTG-3'; GAPDH forward, 5'-ACAACCTTTGGTATCG TGGAAGG-3' and reverse, 5'-GCCATCACGCCACAGTT TC-3'; U6 forward, 5'-CTCGCTTCGGCAGCACATA-3' and reverse, 5'-AACGATTCACGAATTTGCGT-3'.

Western blot analysis. Cell lysates were obtained with RIPA lysis buffer containing 1% protease inhibitor and protein concentrations were determined using a BCA kit (Thermo Fisher Scientific, Inc.). Subsequently, 10 μg protein/lane was detached by 10% SDS-PAGE and transferred to PVDF membranes. After sealing in 5% skim milk for 2 h, the membranes were probed with primary antibodies against Beclin1 (dilution, 1:1,000; #3738, Cell Signaling Technology, Inc.), p62 (dilution 1:1,000; #88588, Cell Signaling Technology, Inc.), Bcl-2

(dilution 1:1,000; #15071, Cell Signaling Technology, Inc.), Bax (dilution 1:1,000; #2774, Cell Signaling Technology, Inc.), HIF1A (dilution 1:1,000; #3716, Cell Signaling Technology, Inc.) and GAPDH (dilution 1:1,000; sc-47724; Santa Cruz Biotechnology, Inc.) at 4°C overnight, followed by incubation with horseradish peroxidase-conjugated secondary antibodies (dilution 1:1,000; goat anti-mouse IgG, ab205719 and goat anti-rabbit IgG, ab205718; Abcam) for 2 h at room temperature and visualized with the enhanced chemiluminescence (ECL) kit (Thermo Fisher Scientific, Inc.). Protein expression was quantified using Image-Pro® Plus software (version 6.0; Media Cybernetics, Inc.).

Bioinformatics analysis and luciferase reporter assays. The starBase database (<http://starbase.sysu.edu.cn/>) was used to predict the potential target genes of circCCDC66. The sequence of the 3'-UTR (untranslated region) of miR-3140 was identified as a novel potential target gene. To evaluate the association between miR-3140 and circCCDC66, a luciferase reporter assay was carried out. The fragments of circCCDC66 containing the speculated miR-3140 binding sites were inserted into the reporter vectors pmiRGLO (Shanghai GenePharma Co., Ltd.) to construct circCCDC66-WT plasmids. The circCCDC66-Mut vectors were synthesized by mutating the sequences of the binding sites. Subsequently, 293T cells were co-transfected with indicated reporter vectors and NC mimic, miR-3140 mimic, NC inhibitor, and miR-3140 inhibitor. At 48 h post-transfection, the Dual Luciferase assay system (Promega Corp.) was utilized to measure the luciferase activity based on the manufacturer's instructions.

Statistical analysis. Data are presented as the mean ± SD of three independent assays. All statistical analyses were carried out with SPSS 17.0 software (SPSS, Inc.). Comparisons of parameters between two groups were analyzed by a paired Student's t-test. Comparisons among multiple groups were performed using one-way ANOVA followed by Tukey's test. All experiments were conducted for three replicates. $P < 0.05$ was considered to indicate a statistically significant difference.

Results

Knockdown of circCCDC66 inhibits the progression of CRC cells. Firstly, we determined the expression of circCCDC66 in CRC tissues and cell lines (HCT116 and SW620). As demonstrated by RT-qPCR, circCCDC66 expression was significantly increased in CRC tissues compared with that in the corresponding normal tissues (Fig. 1A). In addition, circCCDC66 expression was higher in CRC cell lines than that of the NCM460 control (Fig. 1B). To investigate the biological role of circCCDC66 in CRC, HCT116 and SW620 cells were transfected with sh-NC and sh-circCCDC66. The transfection efficiency was confirmed by RT-qPCR (Fig. 1C). Moreover, knockdown of circCCDC66 reduced viability, migration and invasion, and enhanced the apoptosis of CRC cells (Fig. 1D-G). Western blot analysis indicated that circCCDC66 knockdown significantly increased the level of Bax and significantly decreased Bcl-2 expression (Fig. 1H). Overall, the data indicated that circCCDC66 promoted the tumorigenesis of CRC.

Hypoxia contributes to the progression of CRC and upregulates circCCDC66 expression. In order to investigate the role of hypoxia in CRC, HCT116 and SW620 cells were exposed to hypoxia. As a factor closely related to hypoxic changes, hypoxia inducible factor 1 subunit α (HIF1A) mRNA and protein levels were both significantly promoted following exposure to hypoxia (Fig. 2A). Furthermore, RT-qPCR indicated that hypoxia significantly increased the expression of circCCDC66 in CRC cells (Fig. 2B). CCK-8 assay indicated that hypoxia led to a significant increase in cell viability (Fig. 2C). Transwell and wound healing assays demonstrated that exposure to hypoxia facilitated the invasion and migration of HCT116 and SW620 cells (Fig. 2D and E). Consistently, it was observed that the apoptosis of CRC cells was significantly suppressed by hypoxia (Fig. 2F and G). Taken together, these results indicated that hypoxia promoted the progression of CRC and circCCDC66 was upregulated in hypoxia-exposed CRC cells.

Silencing of circCCDC66 suppresses the hypoxia-induced CRC cell phenotype. Subsequently, the present study aimed to investigate the exact function of circCCDC66 in CRC. circCCDC66 expression was knocked down in HCT116 and SW620 cells by transfection with sh-circCCDC66 (Fig. 3A). CCK-8 assay revealed that the depletion of circCCDC66 significantly decreased cell viability following exposure to hypoxia (Fig. 3B). Transwell assay and wound healing assay disclosed that the ability of invasion and migration was suppressed by the downregulation of circCCDC66 in the hypoxia-exposed CRC cells (Fig. 3C and D). Consistently, flow cytometric analysis and western blot analysis illustrated that circCCDC66 knockdown contributed to a significant increase in the apoptosis of the hypoxia-exposed HCT116 and SW620 cells (Fig. 3E and F). Taken together, these results provided strong evidence that the inhibition of circCCDC66 suppresses the hypoxia-induced malignant behaviors of CRC cells.

circCCDC66 functions as a sponge of miR-3140. By using the starBase database, miR-3140 was predicted as a potential downstream target gene of circCCDC66 (Fig. 4A). Luciferase reporter assay delineated that the luciferase activity of wild-type circCCDC66 was impaired by miR-3140 mimic and increased by miR-3140 inhibitor; however, the luciferase activity of mutant circCCDC66 exhibited no response to miR-3140 mimic or inhibitor, which confirmed that circCCDC66 directly bound to miR-3140 (Fig. 4B). Furthermore, the results of RT-qPCR analysis elucidated that the overexpression of miR-3140 significantly diminished the expression of circCCDC66, whereas the depletion of miR-3140 significantly increased the circCCDC66 level (Fig. 4C). In a word, these findings affirmed that miR-3140 was sponged by circCCDC66.

Inhibition of miR-3140 partially abrogates the effects of circCCDC66 knockdown on hypoxia-exposed CRC cells. Thereafter, the present study aimed to validate whether circCCDC66 exerts its function through miR-3140. The results of RT-qPCR revealed that miR-3140 expression was increased by the knockdown of circCCDC66 and restoration of the miR-3140 level occurred following transfection

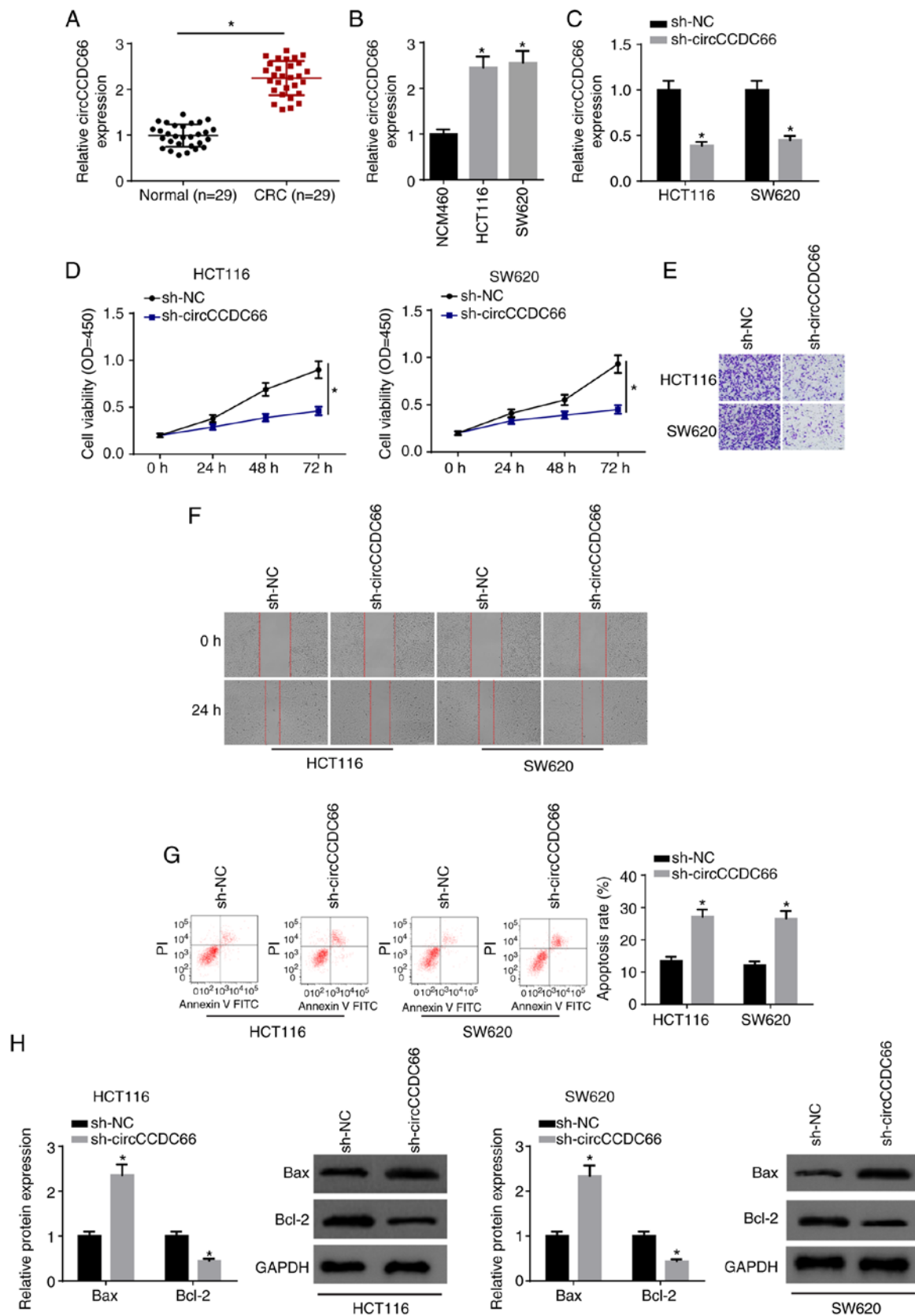


Figure 1. Knockdown of circCCDC66 inhibits the progression of CRC cells. (A) The expression of circCCDC66 in CRC tissues and adjacent non-cancerous tissues was determined by RT-qPCR. * $P < 0.05$ vs. the normal tissues. (B) Expression of circCCDC66 in CRC cell lines (HCT116 and SW620) and human colon mucosal cells (NCM460) was measured by RT-qPCR. * $P < 0.05$ vs. NCM460 cells. (C) Expression of circCCDC66 in HCT116 and SW620 transfected with sh-NC or sh-circCCDC66 was determined by RT-qPCR. * $P < 0.05$ vs. the sh-NC group. (D) CCK-8 assay showed the viability of HCT116 and SW620 cells transfected with sh-NC or sh-circCCDC66. * $P < 0.05$ vs. the sh-NC group. (E and F) Transwell assay and wound healing assay were employed to determine the migratory and invasive abilities of HCT116 and SW620 cells transfected with sh-NC or sh-circCCDC66. (G) Flow cytometry analysis was used to detect the apoptosis of HCT116 and SW620 cells transfected with sh-NC or sh-circCCDC66. * $P < 0.05$ vs. the sh-NC group. (H) The protein levels of Bax and Bcl-2 in HCT116 and SW620 cells transfected with sh-NC or sh-circCCDC66 were detected by western blot analysis. * $P < 0.05$ vs. the sh-NC group. CRC, colorectal cancer.

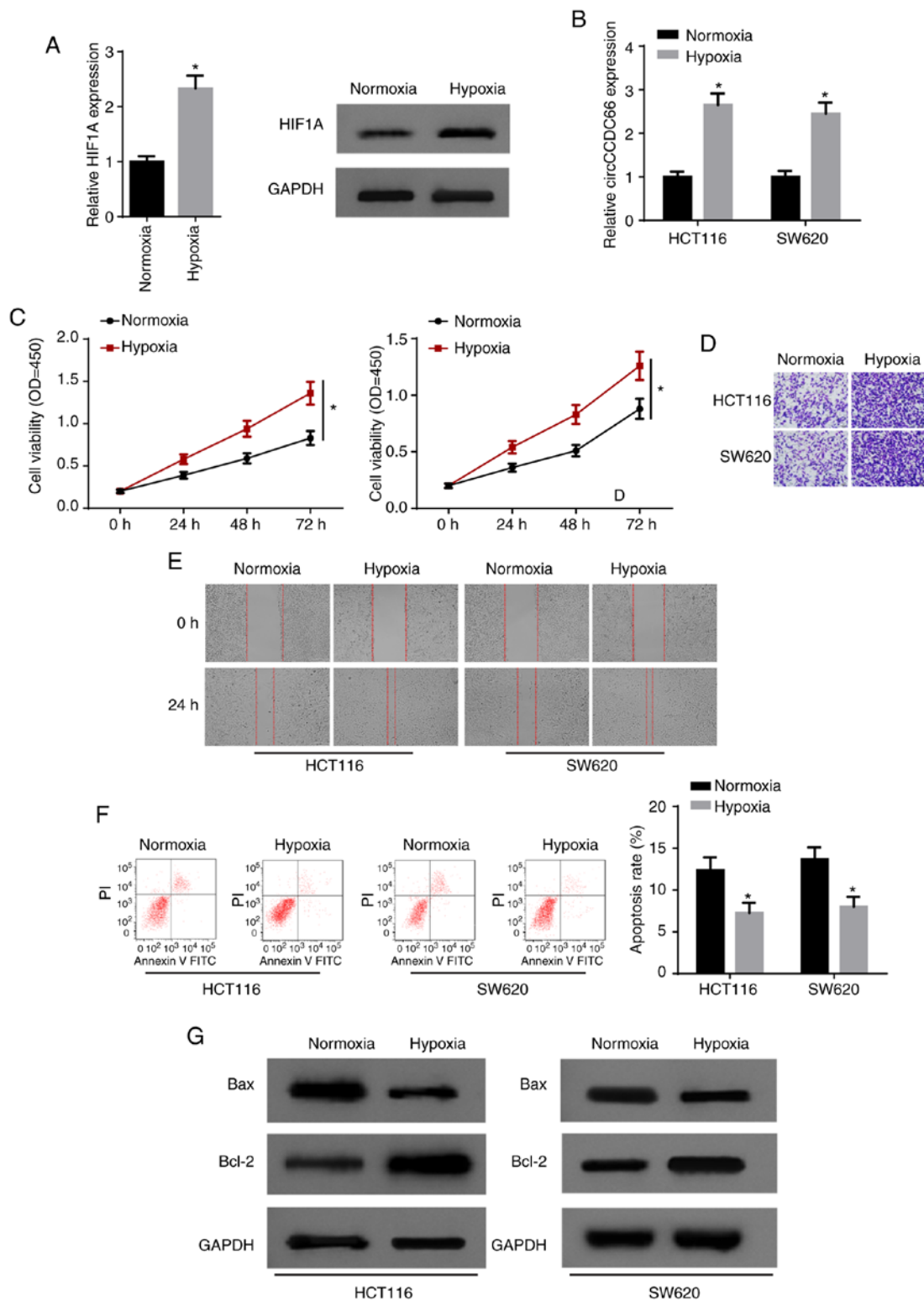


Figure 2. Hypoxia contributes to the progression of CRC and upregulates circCCDC66 expression. (A) HIF1A mRNA and protein levels were measured in hypoxia-exposed HCT116 and SW620 cells by RT-qPCR and western blot analysis. * $P < 0.05$ vs. normoxia. (B) RT-qPCR showed circCCDC66 expression in HCT116 and SW620 cells after hypoxia treatment. * $P < 0.05$ vs. normoxia. (C) The viability of hypoxia-exposed HCT116 and SW620 cells was estimated by CCK-8 assay. * $P < 0.05$ vs. normoxia. (D) Transwell assay was performed to detect cell invasion in hypoxia-exposed HCT116 and SW620 cells. (E) The migration ability of hypoxia-exposed HCT116 and SW620 cells was tested by wound healing assay. (F) The apoptosis rate of hypoxia-exposed HCT116 and SW620 cells analyzed by flow cytometry. * $P < 0.05$ vs. normoxia. (G) The protein levels of Bax and Bcl-2 in hypoxia-exposed CRC cells were detected by western blot analysis. CRC, colorectal cancer; HIF1A, hypoxia inducible factor 1 subunit α .

with miR-3140 inhibitor (Fig. 5A). CCK-8 assay revealed that the viability of hypoxia-exposed HCT116 cells, which was suppressed by circCCDC66 downregulation, was increased by

the inhibition of miR-3140 (Fig. 5B). Moreover, the suppression of the cell invasive and migratory abilities induced by the silencing of circCCDC66 was abolished by transfection with

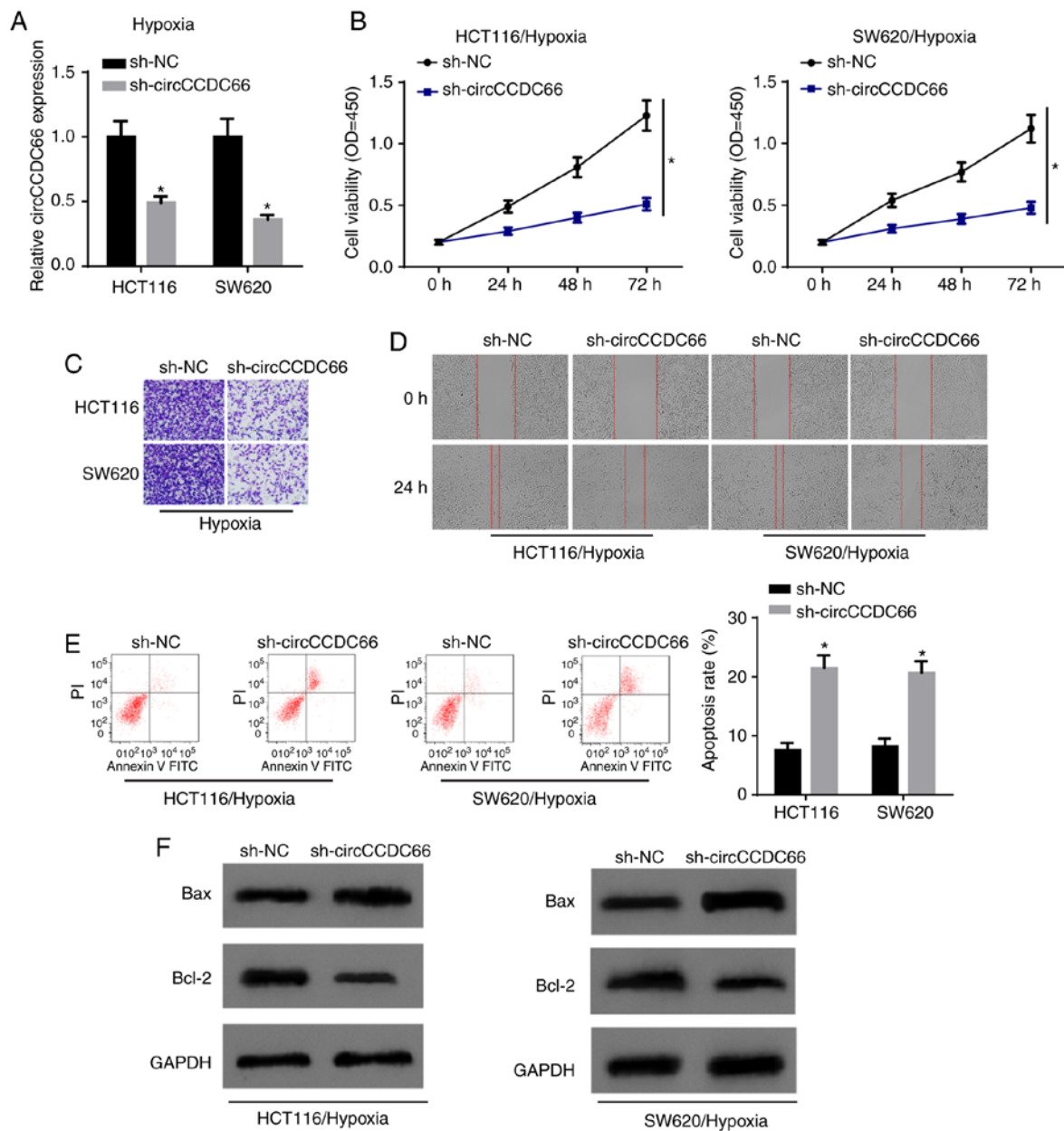


Figure 3. Silencing of circCCDC66 suppresses hypoxia-induced CRC cell phenotype. (A) The efficiency of circCCDC66 knockdown in hypoxia-exposed HCT116 and SW620 cells was verified by RT-qPCR analysis. * $P < 0.05$ vs. the sh-NC group. (B) CCK-8 assay was conducted to examine cell viability in HCT116 and SW620 cells transfected with sh-NC or sh-circCCDC66 after exposure to hypoxia condition. * $P < 0.05$ vs. the sh-NC group. (C and D) The impacts of sh-circCCDC66 on cell invasion and migration of HCT116 and SW620 cells treated with hypoxia were estimated by Transwell assay and wound healing assay. (E) Flow cytometric analysis was used to detect the apoptosis of hypoxia-exposed HCT116 and SW620 cells following circCCDC66 downregulation. * $P < 0.05$ vs. the sh-NC group. (F) The protein levels of Bax and Bcl-2 in hypoxia-exposed CRC cells were detected by western blot analysis. CRC, colorectal cancer.

miR-3140 inhibitor (Fig. 5C and D). In agreement with the above-mentioned findings, flow cytometric analysis and western blot analysis revealed that the increased apoptosis rate following circCCDC66 depletion on cell apoptosis was partly abrogated by the downregulation of miR-3140 in the hypoxia-exposed cells (Fig. 5E and F). Thus, circCCDC66 executed its oncogenic role in hypoxia-exposed CRC cells by regulating miR-3140.

miR-3140 inhibits the autophagy pathway. Considering that autophagy plays a vital role in the development and evolution of malignancies, the association between autophagy and miR-3140 was subsequently investigated. The results of RT-qPCR and western blot analysis revealed that the elevated

expression of miR-3140 resulted in a significant reduction in Beclin1 expression and a significant increase in the p62 level, while the silencing of miR-3140 increased the level of Beclin1 and significantly decreased p62 expression (Fig. 6A and B). Based on these results, it was concluded that miR-3140 led to the suppression of autophagy.

Activation of autophagy recovers the miR-3140-regulated cell phenotype of hypoxia-exposed CRC cells. Rescue experiments were performed to verify the specific function of autophagy in the circCCDC66/miR-3140 axis. CCK-8 assay revealed that the enhanced expression of miR-3140 decreased cell viability and the autophagy inducer rapamycin

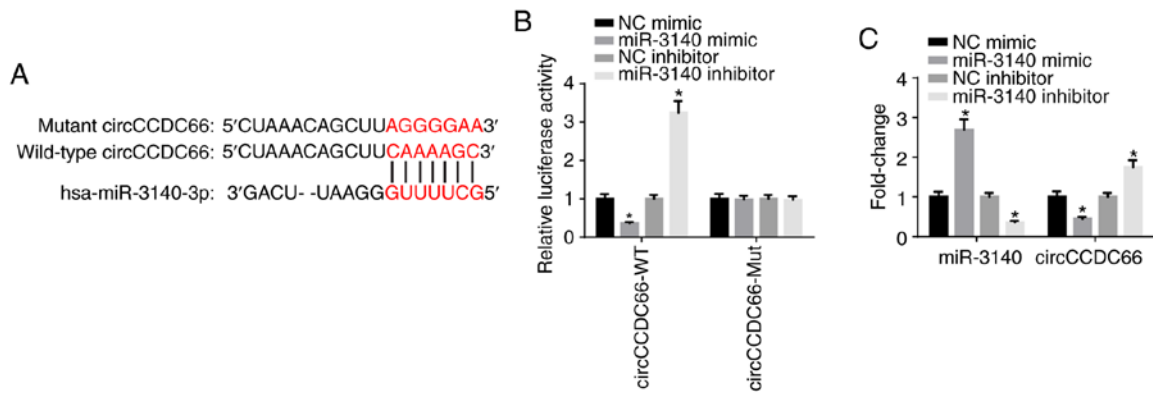


Figure 4. circCCDC66 functions as a sponge of miR-3140. (A) The potential binding sites of circCCDC66 for miR-3140 were predicted by starBase database. (B) Luciferase reporter assay was carried out to investigate the association between circCCDC66 and miR-3140 in 293T cells. (C) RT-qPCR assay was adopted to measure the expression of miR-3140 and circCCDC66 in HCT116 cells transfected with NC mimic, miR-3140 mimic, NC inhibitor or miR-3140 inhibitor. *P<0.05 vs. the NC mimic or NC inhibitor group.

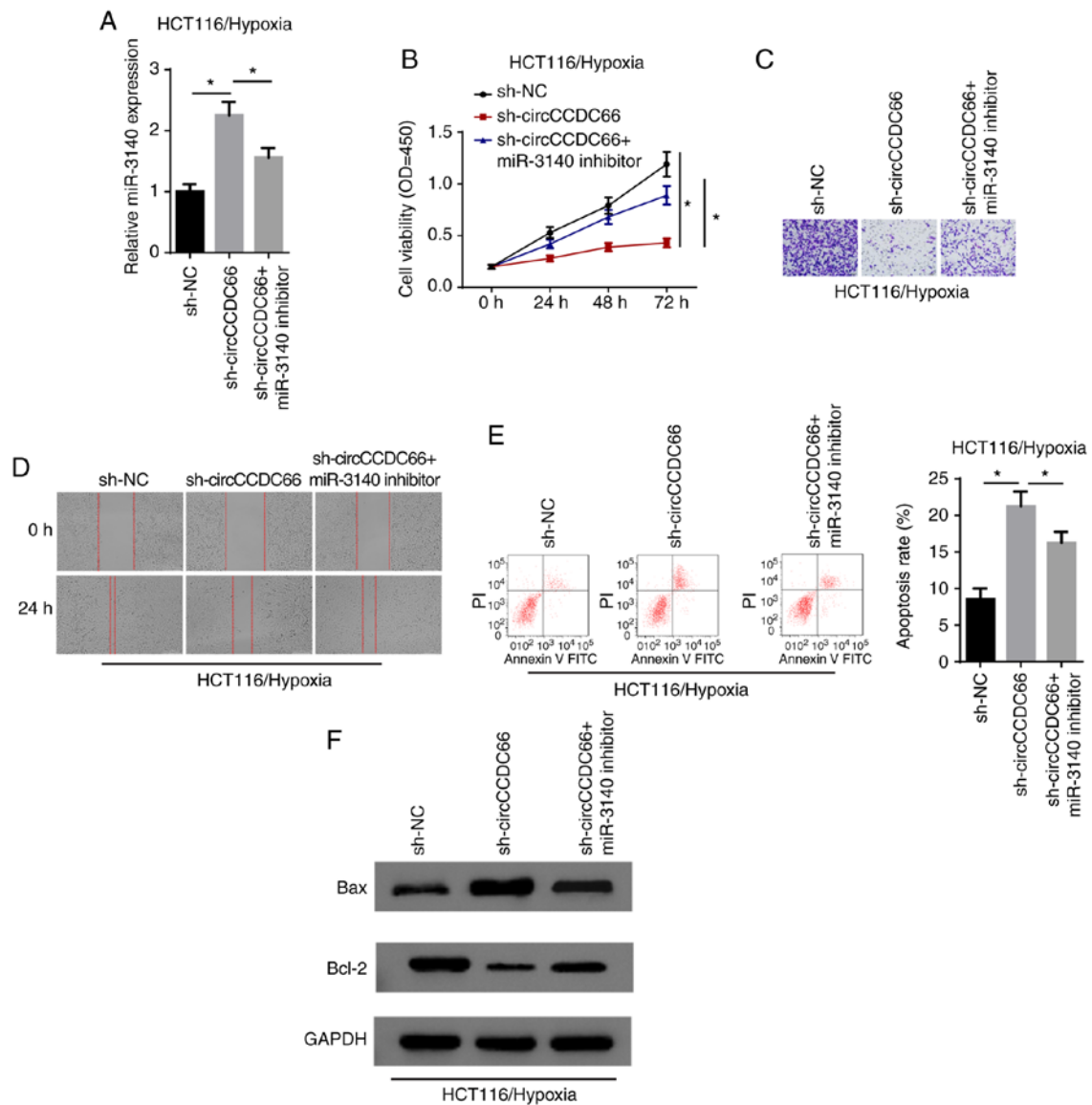


Figure 5. Inhibition of miR-3140 partially abrogates the effects of circCCDC66 knockdown on hypoxia-exposed CRC cells. (A) RT-qPCR showed the expression of miR-3140 in hypoxia-exposed HCT116 cells transfected with sh-NC, sh-circCCDC66, sh-circCCDC66 + miR-3140 inhibitor. *P<0.05. (B) CCK-8 assay showed the viability of hypoxia-exposed HCT116 cells transfected with sh-NC, sh-circCCDC66, sh-circCCDC66 + miR-3140 inhibitor. *P<0.05. (C and D) Transwell and wound healing assays showed the migratory and invasive abilities in HCT116 cells treated with hypoxia. (E) Flow cytometric assay showed the apoptosis rate of hypoxia-exposed HCT116 cells transfected with sh-NC, sh-circCCDC66, sh-circCCDC66 + miR-3140 inhibitor. *P<0.05. (F) The protein levels of Bax and Bcl-2 in hypoxia-exposed HCT116 cells were detected by western blot analysis. CRC, colorectal cancer.

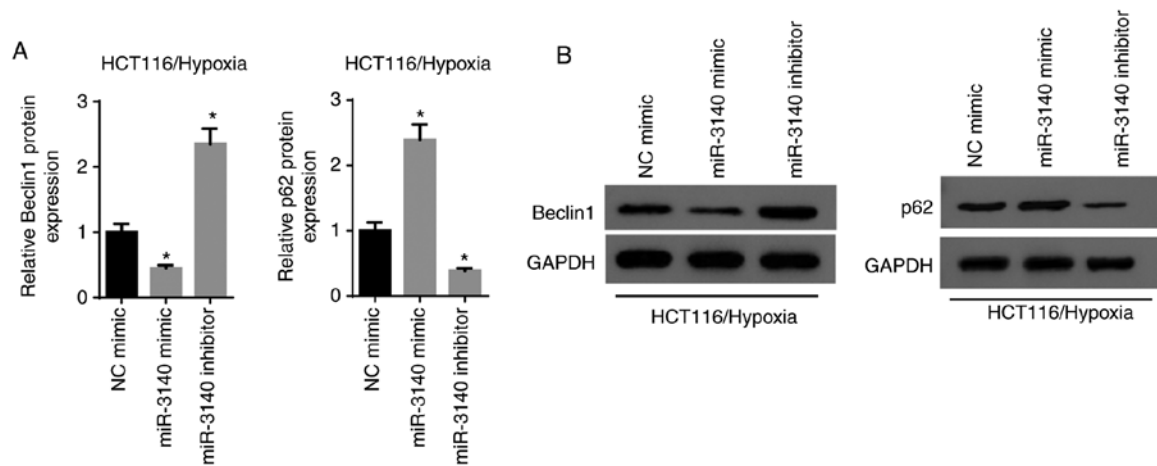


Figure 6. miR-3140 inhibits the autophagy pathway. (A) RT-qPCR results of the expression of autophagy markers Beclin1 and p62 in HCT116 cells transfected with NC, miR-3140 mimic or miR-3140 inhibitor. * $P < 0.05$ vs. the NC mimic group. (B) The protein levels of Beclin1 and p62 were assessed by western blot analysis when miR-3140 was overexpressed or knocked down in HCT116 cells. GAPDH served as the internal reference.

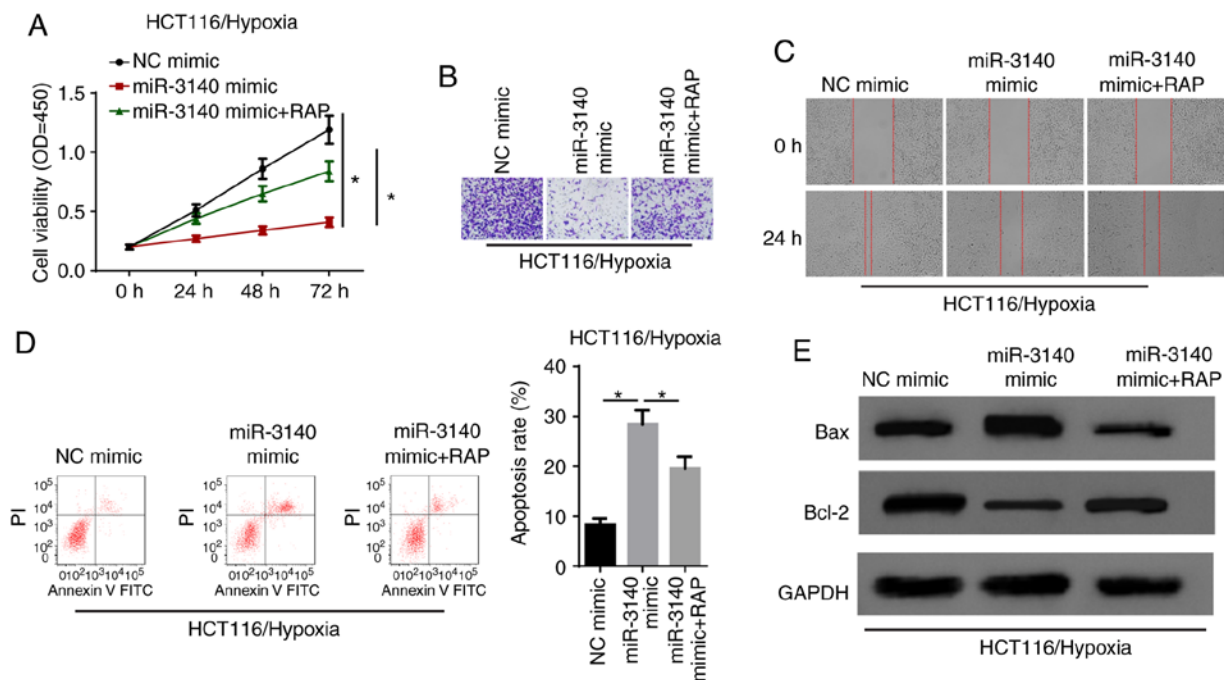


Figure 7. Activation of autophagy recovers the miR-3140-regulated cell phenotype of hypoxia-exposed CRC cells. (A) After hypoxia treatment, the cell viability were analyzed by CCK-8 assay in HCT116 cells transfected with NC mimic, miR-3140 mimic, miR-3140 mimic + RAP. * $P < 0.05$. (B and C) Transwell assay and wound healing assay showed the migration and invasion of HCT116 cells transfected with NC mimic, miR-3140 mimic, miR-3140 mimic + RAP after exposure to hypoxia condition. (D) Flow cytometry assay showed the apoptosis rate of hypoxia-exposed HCT116 cells transfected with NC mimic, miR-3140 mimic, miR-3140 mimic + RAP. * $P < 0.05$. (E) Western blot analysis showed the protein levels of Bax and Bcl-2 in hypoxia-exposed HCT116 cells transfected with NC mimic, miR-3140 mimic, miR-3140 mimic + RAP. CRC, colorectal cancer; RAP, rapamycin.

(RAP) significantly recovered the cell proliferative capability (Fig. 7A). Moreover, it was validated that cell invasion and migration, which were suppressed by the overexpression of miR-3140 were renewed owing to the activation of autophagy (Fig. 7B and C). Additionally, flow cytometric analysis and western blot revealed that cell apoptosis was significantly promoted by miR-3140 upregulation; however, treatment with RAP abolished the effects of miR-3140 ectopic expression on hypoxia-exposed HCT116 cells (Fig. 7D and E). In summary, it was concluded that miR-3140 suppressed the progression of CRC under hypoxic conditions via autophagy.

Discussion

Previous evidence has illuminated that circulating RNAs (circRNAs) act as vital regulators in tumorigenesis and the development of diverse malignancies by modulating different cellular activities (23,24). For example, circRNA_0084043 facilitates malignant melanoma progression via miR-153-3p/Snail axis (25). CircRNA CBL11 inhibits cell proliferation of colorectal cancer by targeting miR-6778-5p in (26). It has been demonstrated that circCCDC66 plays an oncogenic role in colon cancer (13). Consistent with the

previous study, we demonstrated that circCCDC66 expression was upregulated in colorectal cancer (CRC) tissues and cell lines, and knockdown of circCCDC66 inhibited the development and progression of CRC.

Considering that intratumoral hypoxia is one of the driving forces of tumor occurrence and development (27,28), the present study explored the biological role of hypoxia in CRC. The findings revealed that hypoxia induced the progression of CRC by promoting cell viability, invasion and migration, whereas it inhibited cell apoptosis. Furthermore, the exposure of CRC cells to hypoxic conditions increased the expression of circCCDC66. To further explore the involvement of circCCDC66 in hypoxia-induced CRC, loss-of-function assays were performed under hypoxic conditions. The results revealed that the depletion of circCCDC66 inhibited hypoxia-exposed CRC cell growth and metastasis. Moreover, the competing endogenous (ceRNA) network exhibits its regulatory function in human cancer, and circRNAs can function as ceRNAs, playing a role in the regulation of cancer (29-32). For example, circ-0001313 promotes the development and progression of colon cancer by acting as a ceRNA through sponging miR-510 and regulating AKT2 (33). circ_0007843 promotes colon cancer tumorigenesis by downregulating miR-518c (34). In the present study, it was found that circCCDC66 inhibited miR-3140 expression via direct interaction. Additionally, the inhibition of miR-3140 partly abolished the effects of circCCDC66 downregulation on hypoxia-exposed CRC cells.

Autophagy, a highly conservative process of cell self-degradation, generally appears in a wide spectrum of cancer cells (35). Previous studies have demonstrated that autophagy is activated in response to hypoxia and other types of stress, and the activation of autophagy contributes to the tumorigenesis of numerous malignancies, including CRC. For example, hypoxia-induced autophagy promotes the occurrence and progression of CRC via the PRKC/PKC-EZR pathway (36). Che *et al* reported that miR-20a suppressed hypoxia-induced autophagy by targeting ATG5/FIP200 in CRC (37). Therefore, to gain a better understanding of the molecular regulatory mechanisms underlying circCCDC66, the present study examined the association between miR-3140 and autophagy. The experimental data indicated that miR-3140 suppressed autophagy and the activation of autophagy by RAP renewed the miR-3140-regulated cell phenotype of hypoxia-exposed CRC cells.

In conclusion, the present study, to the best of our knowledge, is the first to demonstrate that circCCDC66 activates autophagy to facilitate CRC progression under hypoxic conditions by sponging miR-3140, which provides a novel therapeutic strategy for CRC. However, some limitations remain to be further addressed: First, the regulatory mechanisms of circCCDC66/miR-3140 in CRC *in vivo* warrant further investigation. Secondly, the other downstream effectors of circCCDC66 should be investigated in future studies. Thirdly, the specific regulatory mechanisms of miR-3140 in the modulation of autophagy remain to be clarified. In addition, further studies are required to identify the target genes of miR-3140 which are responsible for its association with autophagy.

Acknowledgements

Not applicable.

Funding

This work was supported by the Applied Basic Research Project of Changzhou Science and Technology Bureau (no. CJ20180070) and Changzhou High-Level Medical Talents Training Project (no. 2016-CZBJ046).

Availability of data and materials

The datasets used and/or analyzed during the present study are available from the corresponding author on reasonable request.

Authors' contributions

JF, ZL and XH designed the present study. LL and HX performed the experiments. QL and JF analyzed the data and prepared the figures. JF and XH drafted the initial manuscript. XH reviewed and revised the manuscript. All authors read and approved the manuscript and agree to be accountable for all aspects of the research in ensuring that the accuracy or integrity of any part of the work are appropriately investigated and resolved.

Ethics approval and consent to participate

Written informed consent was obtained from all patients prior to the study start. The present study was approved by the First People's Hospital of Changzhou (Changzhou, Jiangsu, China).

Patient consent for publication

Not applicable.

Competing interests

The authors declare that they have no competing interests.

References

1. Siegel RL, Miller KD and Jemal A: Cancer statistics, 2015. *CA Cancer J Clin* 65: 5-29, 2015.
2. Brenner H, Kloor M and Pox CP: Colorectal cancer. *Lancet* 383: 1490-1502, 2014.
3. Bruera G and Ricevuto E: Intensive chemotherapy of metastatic colorectal cancer: Weighing between safety and clinical efficacy: Evaluation of Masi G, Loupakis F, Salvatore L, *et al*: Bevacizumab with FOLFOXIRI (irinotecan, oxaliplatin, fluorouracil, and folinate) as first-line treatment for metastatic colorectal cancer: A phase 2 trial. *Lancet Oncol* 11: 845-852, 2010. *Expert Opin Biol Ther* 11: 821-814, 2011.
4. Petrelli F and Barni S: Correlation of progression-free and post-progression survival with overall survival in advanced colorectal cancer. *Ann Oncol* 24: 186-192, 2013.
5. Zheng H, Wu Y, Guo T, Liu F, Xu Y and Cai S: Hypoxia induces growth differentiation factor 15 to promote the metastasis of colorectal cancer via PERK-eIF2 α signaling. *Biomed Res Int* 2020: 5958272, 2020.
6. Choi BJ, Park SA, Lee SY, Cha YN and Surh YJ: Hypoxia induces epithelial-mesenchymal transition in colorectal cancer cells through ubiquitin-specific protease 47-mediated stabilization of Snail: A potential role of Sox9. *Sci Rep* 7: 15918, 2017.
7. Guo JU, Agarwal V, Guo H and Bartel DP: Expanded identification and characterization of mammalian circular RNAs. *Genome Biol* 15: 409, 2014.
8. Barrett SP, Wang PL and Salzman J: Circular RNA biogenesis can proceed through an exon-containing lariat precursor. *Elife* 4: e07540, 2015.

9. Liang H, Huang H, Li Y, Lu Y and Ye T: CircRNA_0058063 functions as a ceRNA in bladder cancer progression via targeting miR-486-3p/FOXp4 axis. *Biosci Rep* 40: BSR20193484, 2020.
10. Hu K, Qin X, Shao Y, Zhou Y, Ye G and Xu S: Circular RNA MTO1 suppresses tumorigenesis of gastric carcinoma by sponging miR-3200-5p and targeting PEBP1. *Mol Cell Probes* 52: 101562, 2020.
11. Bian L, Zhi X, Ma L, Zhang J, Chen P, Sun S, Li J, Sun Y and Qin J: Hsa_circRNA_103809 regulated the cell proliferation and migration in colorectal cancer via miR-532-3p/FOXO4 axis. *Biochem Biophys Res Commun* 505: 346-352, 2018.
12. Zeng K, Chen X, Xu M, Liu X, Hu X, Xu T, Sun H, Pan Y, He B and Wang S: CircHIPK3 promotes colorectal cancer growth and metastasis by sponging miR-7. *Cell Death Dis* 9: 417, 2018.
13. Hsiao KY, Lin YC, Gupta SK, Chang N, Yen L, Sun HS and Tsai SJ: Noncoding effects of circular RNA CCDC66 promote colon cancer growth and metastasis. *Cancer Res* 77: 2339-2350, 2017.
14. Wei Y, Zhang Y, Meng Q, Cui L and Xu C: Hypoxia-induced circular RNA has_circRNA_403658 promotes bladder cancer cell growth through activation of LDHA. *Am J Transl Res* 11: 6838-6849, 2019.
15. Ren S, Liu J, Feng Y, Li Z, He L, Li L, Cao X, Wang Z and Zhang Y: Knockdown of circDENND4C inhibits glycolysis, migration and invasion by up-regulating miR-200b/c in breast cancer under hypoxia. *J Exp Clin Cancer Res* 38: 388, 2019.
16. Turchinovich A, Weiz L and Burwinkel B: Extracellular miRNAs: The mystery of their origin and function. *Trends Biochem Sci* 37: 460-465, 2012.
17. Thomou T, Mori MA, Dreyfuss JM, Konishi M, Sakaguchi M, Wolfrum C, Rao TN, Winnay JN, Garcia-Martin R, Grinspoon SK, *et al*: Adipose-derived circulating miRNAs regulate gene expression in other tissues. *Nature* 542: 450-455, 2017.
18. Sun N, Zhang L, Zhang C and Yuan Y: miR-144-3p inhibits cell proliferation of colorectal cancer cells by targeting BCL6 via inhibition of Wnt/ β -catenin signaling. *Cell Mol Biol Lett* 25: 19, 2020.
19. Weihua Z, Guorong Z, Xiaolong C and Weizhan L: MiR-33a functions as a tumor suppressor in triple-negative breast cancer by targeting EZH2. *Cancer Cell Int* 20: 85, 2020.
20. Fang QY, Deng QF, Luo J and Zhou CC: MiRNA-20a-5p accelerates the proliferation and invasion of non-small cell lung cancer by targeting and downregulating KLF9. *Eur Rev Med Pharmacol Sci* 24: 2548-2556, 2020.
21. Tonouchi E, Gen Y, Muramatsu T, Hiramoto H, Tanimoto K, Inoue J and Inazawa J: miR-3140 suppresses tumor cell growth by targeting BRD4 via its coding sequence and downregulates the BRD4-NUT fusion oncoprotein. *Sci Rep* 8: 4482, 2018.
22. Livak KJ and Schmittgen TD: Analysis of relative gene expression data using real-time quantitative PCR and the 2(-Delta Delta C(T)) method. *Methods* 25: 402-408, 2001.
23. Dong Y, He D, Peng Z, Peng W, Shi W, Wang J, Li B, Zhang C and Duan C: Circular RNAs in cancer: An emerging key player. *J Hematol Oncol* 10: 2, 2017.
24. Meng S, Zhou H, Feng Z, Xu Z, Tang Y, Li P and Wu M: CircRNA: Functions and properties of a novel potential biomarker for cancer. *Mol Cancer* 16: 94, 2017.
25. Luan W, Shi Y, Zhou Z, Xia Y and Wang J: CircRNA_0084043 promote malignant melanoma progression via miR-153-3p/Snail axis. *Biochem Biophys Res Commun* 502: 22-29, 2018.
26. Li H, Jin X, Liu B, Zhang P, Chen W and Li Q: CircRNA CBL11 suppresses cell proliferation by sponging miR-6778-5p in colorectal cancer. *BMC Cancer* 19: 826, 2019.
27. Kim CW, Oh ET, Kim JM, Park JS, Lee DH, Lee JS, Kim KK and Park HJ: Hypoxia-induced microRNA-590-5p promotes colorectal cancer progression by modulating matrix metalloproteinase activity. *Cancer Lett* 416: 31-41, 2018.
28. Ullmann P, Nurmik M, Schmitz M, Rodriguez F, Weiler J, Qureshi-Baig K, Felten P, Nazarov PV, Nicot N, Zuegel N, *et al*: Tumor suppressor miR-215 counteracts hypoxia-induced colon cancer stem cell activity. *Cancer Lett* 450: 32-41, 2019.
29. Zhang L, Song X, Chen X, Wang Q, Zheng X, Wu C and Jiang J: Circular RNA CircCACTIN promotes gastric cancer progression by sponging miR-331-3p and regulating TGFBR1 expression. *Int J Biol Sci* 15: 1091-1103, 2019.
30. Wei S, Zheng Y, Jiang Y, Li X, Geng J, Shen Y, Li Q, Wang X, Zhao C, Chen Y, *et al*: The circRNA circPTPRA suppresses epithelial-mesenchymal transitioning and metastasis of NSCLC cells by sponging miR-96-5p. *EBioMedicine* 44: 182-193, 2019.
31. Hansen TB, Jensen TI, Clausen BH, Bramsen JB, Finsen B, Damgaard CK and Kjems J: Natural RNA circles function as efficient microRNA sponges. *Nature* 495: 384-388, 2013.
32. Sumazin P, Yang X, Chiu HS, Chung WJ, Iyer A, Llobet-Navas D, Rajbhandari P, Bansal M, Guarnieri P, Silva J and Califano A: An extensive microRNA-mediated network of RNA-RNA interactions regulates established oncogenic pathways in glioblastoma. *Cell* 147: 370-381, 2011.
33. Tu FL, Guo XQ, Wu HX, He ZY, Wang F, Sun AJ and Dai XD: Circ-0001313/miRNA-510-5p/AKT2 axis promotes the development and progression of colon cancer. *Am J Transl Res* 12: 281-291, 2020.
34. He JH, Han ZP, Luo JG, Jiang JW, Zhou JB, Chen WM, Lv YB, He ML, Zheng L, Li YG and Zuo JD: Hsa_Circ_0007843 acts as a miR-518c-5p sponge to regulate the migration and invasion of colon cancer SW480 cells. *Front Genet* 11: 9, 2020.
35. Ouyang L, Shi Z, Zhao S, Wang FT, Zhou TT, Liu B and Bao JK: Programmed cell death pathways in cancer: A review of apoptosis, autophagy and programmed necrosis. *Cell Prolif* 45: 487-498, 2012.
36. Qureshi-Baig K, Kuhn D, Viry E, Pozdeev VI, Schmitz M, Rodriguez F, Ullmann P, Koncina E, Nurmik M, Frasquilho S, *et al*: Hypoxia-induced autophagy drives colorectal cancer initiation and progression by activating the PRKC/PKC-EZR (ezrin) pathway. *Autophagy*: Jan 17, 2019 (Epub ahead of print).
37. Che J, Wang W, Huang Y, Zhang L, Zhao J, Zhang P and Yuan X: miR-20a inhibits hypoxia-induced autophagy by targeting ATG5/FIP200 in colorectal cancer. *Mol Carcinog* 58: 1234-1247, 2019.



This work is licensed under a Creative Commons Attribution-NonCommercial-NoDerivatives 4.0 International (CC BY-NC-ND 4.0) License.